Experimental Investigations of Parameters Influence on Total Damping Force in MR Fluid Base Damper

Hamir Sapramer, Dr. S. P. Bhatnagar, Dr. G. D. Acharya

Sir Bhavsinhaji Polytechnic Institute, Gujarat Technological University, Ahmedabad, India

***Abstract*— A magnetorheological fluid composition having a magnetisable carrier medium loaded with magnetisable particles to provide a magnetorheological fluid exhibiting enhance rheological properties. Also disclosed in a magnetic particle damper utilizing the magnetorheological fluid composition.**

Magnetorheological (MR) dampers are one of the most advantageous control devices for mechanical engineering applications due to many good features such as small power requirement, reliability, and low price to manufacture. The smart passive system (semi active control system) consists of an MR damper and an electromagnetic induction (EMI) system that uses a permanent magnet and a coil. According to the Faraday law of induction, the EMI system that is attached to the MR damper can produce electric energy and the produced energy is applied to the MR damper to vary the damping characteristics of the damper. Thus, the smart passive system does not require any power at all. Besides the output of electric energy is proportional to input loads due to vibration, which means the smart passive system has adaptability by itself without any controller or sensors.

In the present study, an attempt has been made to investigate the effect of velocity, amplitude and current on total damping force in MR fluid base damper developed at Physics Department, Shri M.K. Bhavnagar University. The experiments were conducted based on response surface methodology (RSM) and sequential approach using face cantered central composite design. The results show that all the factors (piston velocity, Amplitude and Current) has significant effect on Total Damping Force. A linear model best fits the variation of total damping force with velocity, amplitude and current. Current is the dominant contributor to the total damping force. A non-linear quadratic model best describes the variation of total damping force with major contribution of all parameters. The suggested models of total damping force adequately map within the limits of the parameters considered.

***Keywords*— DOE, MR fluid, Damper, Damping force, Dynamic range**

I. INTRODUCTION

Vibration suppression is considered as a key research field in engineering to ensure the safety and comfort of their occupants and users of mechanical structures. To reduce the system vibration, an effective vibration control with isolation is necessary. Vibration control techniques have classically been categorized into two areas, namely passive and active controls. For a long time, efforts were made to improve the effectiveness of the suspension system by optimizing its parameters, but due to the intrinsic limitations of a passive suspension system, improvements were effective only in a certain frequency range. Compared with passive suspensions, active suspensions can improve the performance of the suspension system over a wide range of frequencies. Semi-active suspensions were proposed in the early 1970s [1], and can be nearly as effective as active suspensions. When the control system fails, the semi-active suspension can still work under passive conditions. Compared with active and passive suspension systems, the semi-active suspension system combines the advantages of both active and passive suspensions because it provides better performance when compared with passive suspensions and is economical, safe and does not require either higher-power actuators or a large power supply as active suspensions do [2].

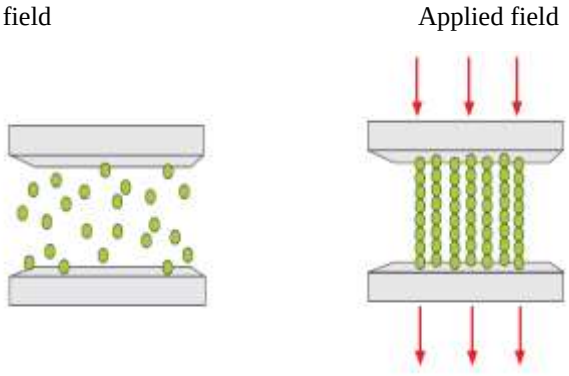

Figure 1: Chain-like structure formation in controllable fluids

The initial discovery and development of MR fluid can be credited to Jacob Rainbow at the US National Bureau of Standards in the late 1940s [6, 7]. These fluids are suspensions of micron-sized, magnetisable particles in an appropriate carrier liquid [8-12]. Normally, MR fluids are free flowing liquids having consistency similar to that of motor oil. However, in the presence of applied magnetic field, the iron particles acquire a dipole moment aligned with the external field which causes particles to form linear chains parallel to the field, as shown in Fig. 1. This phenomenon can solidify the suspended iron particles and restrict the fluid movement. Consequently, yield strength is developed within the fluid. The degree of change is related to the magnitude of the applied magnetic field, and can occur only in a few milliseconds. A typical MR fluid contains 20-40% [5] by volume of relatively pure, soft iron particles, e.g., carbonyl

iron. These particles are suspended in mineral oil, synthetic oil, water or glycol. A variety of proprietary additives similar to those found in commercial lubricant are commonly added to discourage gravitational settling and promote suspension, enhance lubricity, modify viscosity, and inhibit wear. Recently developed MR fluids appear to be attractive alternative for designing of semi active system (controllable fluid dampers) compared to other smart fluids. [6-12]. Magneto rheological (MR) fluids possess rheological properties, which can be changed in a controlled way. These rheological changes are reversible and dependent on the strength of excited magnetic field. MR fluids have potential beneficial applications when placed in various applied loading (shear, valve and squeeze) modes. The squeeze mode is a geometric arrangement where an MR fluid is sandwiched between two flat parallel solid surfaces facing each other. The distance between these two parallel surfaces is called the gap size. These surfaces are either pushed towards or pulled apart from each other by orthogonal magnetic-induced force.

The ultimate strength of an MR fluid depends on the square of the saturation magnetization of the suspended particles. The key to a strong MR fluid is to choose a particle with a large saturation magnetization. The best practical particles are simply pure iron, as they have saturation magnetization of 2.15 Tesla. Typically, the diameter of the magnetisable particles is 3 to 10 microns. Functional MR fluids may be made with larger particles; however, particle suspension becomes increasingly more difficult as the size increases. Smaller particles which are easier to suspend could be used, but the manufacturing of such particles is difficult. Due to the special behaviour of MR fluid, it is used for vast applications such as: dampers, shock absorbers, rotary brakes, clutches, prosthetic devices, polishing and grinding devices, etc. Among them, MR fluid dampers are widely used because of their mechanical simplicity, high dynamic range (Ratio of Controllable force to uncontrollable force), low power requirements, large force capacity and robustness. This class of device has shown to match well with application demands and constraints to offer an attractive means of protecting various engineering systems against interrupted force. MR dampers are being developed for a wide variety of applications where controllable damping is desired. MR damper which utilize the advantages of MR fluids, are semi-active control devices and is popular topic for researchers. A typical MR damper includes MR fluid, a pair of wires, housing, a piston, a magnetic coil and an accumulator as displayed in Fig. 2a. Here, the MR fluid is housed within the cylinder and flows through a small orifice. The magnetic coil is built in the piston or on the housing. When a current is supplied to the coil, the particles are aligned and the fluid changes from the liquid state to the semi-solid state within milliseconds. Consequently, the controllable damping force is produced. The force produced by a MR damper depends on magnetic field induced by the current in the damper coil and the piston velocity as in Fig. 2b.

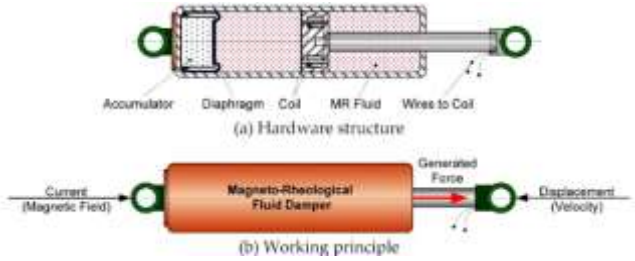

Figure 2. General configuration of a MR fluid damper.

It is capable of generating the force with magnitude sufficient for rapid response in large scale applications [13-15], with requirement only a battery for power [10]. Additionally, these devices offer highly reliable operations and their performance is relatively insensitive to temperature fluctuations or impurities in the fluid [9]. As a result, there has been active research and development of MR fluid dampers and their applications [6-18, 20-21].

The controllable force and the dynamic range are two of the most important parameters in evaluating the overall performance of the MR damper. As illustrated in Fig. 3, the total damper force can be decomposed into a controllable force F_τ due to controllable yield stress and an uncontrollable forceF_{uc}. The uncontrollable force includes a plastic viscous force F_η and a friction F_f. The dynamic range (D) is defined as the ratio between the damper controllable force F_τ and the uncontrollable force F_{uc} as follows:

$$D = \frac{F_\tau}{F_{uc}} = \frac{F_\tau}{F_\eta + F_f}$$

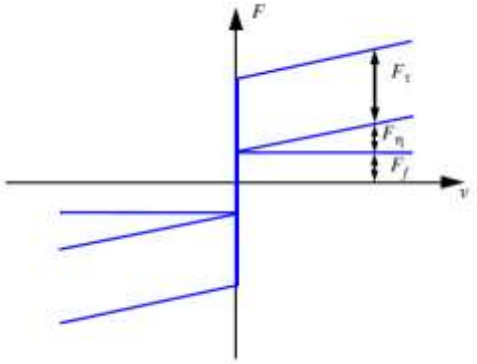

Figure 3: Conceptual design for the MR damper and the EMI part

Most of the experimental investigations on damping force have been conducted using two-level factorial design (2k) for studying influence of parameters on total damping forces. In two-level factorial design, one can identify and model linear relationships only. For studying the nonlinearity present in the output characteristics at least three levels of each factor are required (i.e. three-level factorial design, 3k). A central composite design which requires fewer experiments than alternative 3k design is usually better [19]. Again, sequential experimental approach in central composite design can be used to reduce the number of experiments required. Keeping

the foregoing in mind, the present work is focused on investigations of total damping force as a function of amplitude, velocity and current value using sequential approach in central composite design. The study was conducted on MR damper developed at physics department, Shri M. K. Bhavnagar University, Bhavnagar.

II. ENXPERIMENTAL DETAILS

The details of experimental conditions, instrumentations and measurements and the procedure adopted for the study are described in this section.

A. Magneto Rheological Fluid (MR Fluid)

The magneto rheological fluid developed in house was used in the prototype. The fluid is a suspension of a 10 micron diameter sized magnetically susceptible particles, in Castrol oil carrier fluid. According to the data available by testing this MR fluid on rheometer at this laboratory, the density of the liquid is around 3 g/cm^3 and off state viscosity of a 3.5 Pas. The maximum yield stress value is 15 kPa and it is achieved with the magnetic induction of 0.7 T. When exposed to a magnetic field, the rheology of the fluid reversibly and instantaneously changes from a free-flowing liquid to a semi-solid state with the controllable yield strength as a consequence of the sudden change in the particles arrangement. Figure 4 shows the detail relations of magnetic flux density, viscosity and shear stress available from rheometer.

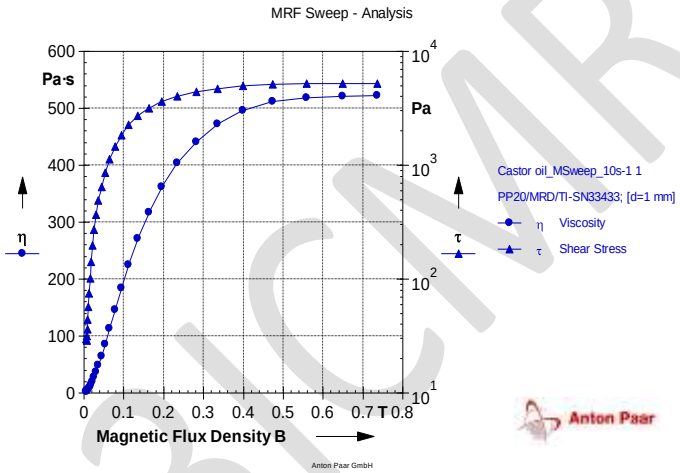

Figure 4. Relation between Magnetic flux density, Viscosity and Shear stress

B. MR Fluid base Damper

The damper is made up of two principal components: housing and piston. Housing contains a volume of magnetorheological (MR) fluid. One fluid which has shown itself to be particularly well-suited for this application consists of carbonyl iron particles suspended in castor oil. Housing is a cylindrical tube with a first closed end with an accumulator and attachment eye associated therewith. A second or open end of the cylinder is closed by upper end cap. A seal is provided to prevent fluid leakage from housing. Accumulator is necessary to accommodate fluid displaced by piston rod as well as to allow for thermal expansion of the fluid. Piston head is spool shaped having an upper outwardly extending flange and a lower outwardly extending flange. Coil is wound upon spool-shaped piston head between upper flange and lower flange. Piston head is made of a magnetically permeable material, in this case, low carbon steel. Guide rails are attached above and below side of piston to keep the piston in centring position to housing during operation. Piston head is formed with a smaller maximum diameter (in this case, D_{pole}) than the inner diameter, D_i of housing. The external surfaces of guides are contoured to engage the inner diameter Di of housing. Guides are made of non-magnetic material, in this case, bronze, and it maintains piston centred within gap 'g'. In this model, gap g (in conjunction with coil) functions as a valve to control the flow of MR fluid past piston. Electrical connection is made to coil through piston rod by lead wires. A first wire is connected to a first end of an electrically conductive rod which extends through piston rod to outside of damper. The second end of the windings of coil is attached to a "ground" connection on the outside of damper. The upper end of piston rod has threads formed thereon to permit attachment of damper, as depicted in figure. An external power supply, which provides a current in the range of 0-4 amps at a voltage of 12-24 volts, is connected to the leads. The outer surface of coil is coated with epoxy paint as a protective measure. The damper of this experiment functions as a Bingham type damper, i.e., this configuration approximates an ideal damper in which the force generated is independent of piston velocity and large forces can be generated with low or zero velocity. This independence improves controllability of the damper making the force a function of the magnetic field strength, which is a function of current flow in the circuit.

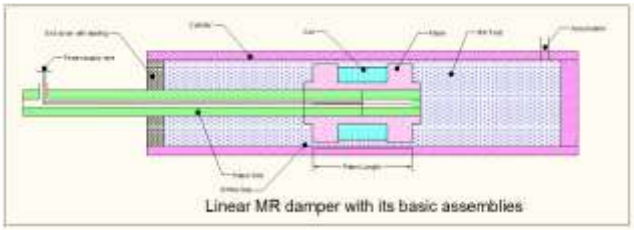

Figure 5. Basic assembly of proposed MR Damper

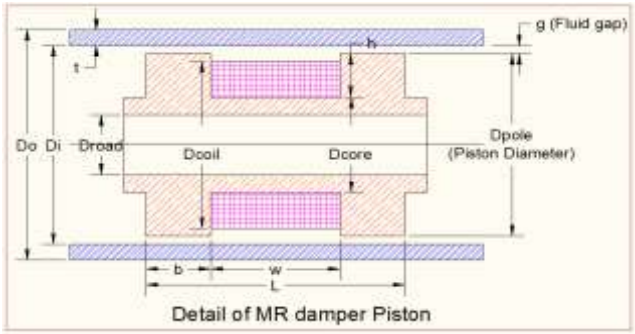

Figure 6. Details of proposed MR Damper Piston

The linear damper prototype is presented as a blueprint in Figure 5. Details of MR damper piston is shown in Figure 6.

C. Total Damping Force Measurement

The shock absorber is characterized by its instantaneous value of position velocity, acceleration, force, pressure, temperature etc. and various plots among these parameters. For the measurement of listed parameters of the shock absorber a test rig is designed and developed. An experiment on the test rig is carried out at different speeds and loads which lead to the output in terms of sinusoidal waveform on attached oscilloscope. The waveform is used to find out the characteristics at different load-speed combination. The results obtained are used to find out the behaviour of shock absorber at different speed and loads.

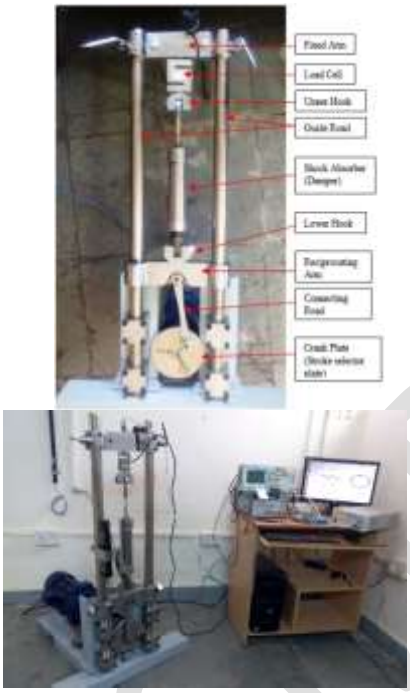

Figure 7. Shock absorber test rig

Figure 7 indicates details of shock absorber test rig setup. The setup consist of Piston and crank (Single Slider Crank Mechanism). This mechanism consists of a crank, connecting rod and piston (reciprocating arm). The crank plate has holes drilled to achieve different stroke lengths shown in figure 7. The advantage of this mechanism is its cost effectiveness because there is less high tolerance machining. The frequency is adjusted by using variable gear drive system based electric motor. The output from the motor is geared down using gearbox. The maximum output shaft speed is in the range of 350 to 400 RPM at full speed of motor having 1440 RPM. Variation

of stroke is possible by fixing the connecting road in appropriate hole made in crank plate, so the stroke is set to give the desired maximum speed within the limits of the damper and test apparatus. There are twelve screwed holes located over spiral shape; connecting rod can be fixed in suitable hole to select stroke length. The longer the stroke, the greater the power needed on motor to move the shock absorber

D. Experimental plan procedure

Thirty two experimental runs composed of 23 factorial points, four centre points and five axial points were carried out in block 1. Table 2 shows complete design matrix with responses to total damping force. In design matrix, the coded variables were arranged as follows: A: amplitude (A), B: angular speed (N) and C: current (I). F is the responses representing total damping force. The experiments were conducted randomly as shown in design matrix ('runs' column in Table 2). The design matrix also, shows the factorial points, centre points and axial points with coded and actual values.

Table 1 – Parameters and their levels

Factor	Unit	Low level (-1)	Centre level (0)	High level (1)
Amplitude	mm	5	10	15
Angular speed	RPM	60	90	120
Current	Amp	0	0.5	1.0

The Model F-value (Table-3) of 255.862 implies the model is significant. There is only a 0.01% chance that a "Model F-Value" this large could occur due to noise. Values of "Prob > F" less than 0.05 indicate model terms are significant. In this case A, B, C and AB are significant model terms. Values greater than 0.05 indicate the model terms are not significant. The "Pred R-Squared" of 0.976504 is in reasonable agreement with the "Adj R-Squared" of 0.986665. "Adeq Precision" measures the signal to noise ratio. A ratio greater than 4 is desirable. The ratio of 67.89797 indicates an adequate signal. This model can be used to navigate the design space.

Table 2 – Design matrix with responses (Total Damping Force)

Std	Run	Block	Type	A:A(mm)	B:N(rpm)	C:I(Amp)	A:A(mm)	B:N(rpm)	C:I(Amp)	F(N)
1	5	1	Axial	0	0	-1	10	90	0	805
2	16	1	Fact	-1	1	0	5	120	0.5	907
3	29	1	Centre	0	0	0	10	90	0.5	1080
4	14	1	Centre	0	0	0	10	90	0.5	1080

5	20	1	Fact	0	-1	1	10	60	1	1215
6	8	1	Fact	0	1	-1	10	120	0	960
7	12	1	Fact	1	-1	0	15	60	0.5	1124.5
8	13	1	Axial	-1	0	0	5	90	0.5	794
9	4	1	Fact	-1	0	-1	5	90	0	510
10	19	1	Fact	-1	-1	1	5	60	1	958
11	17	1	Axial	0	1	0	10	120	0.5	1205
12	27	1	Fact	1	1	1	15	120	1	2070
13	10	1	Fact	-1	-1	0	5	60	0.5	638
14	32	1	Centre	0	0	0	10	90	0.5	1080
15	7	1	Fact	-1	1	-1	5	120	0	616
16	30	1	Centre	0	0	0	10	90	0.5	1080
17	26	1	Fact	0	1	1	10	120	1	1492
18	18	1	Fact	1	1	0	15	120	0.5	1803
19	25	1	Fact	-1	1	1	5	120	1	1263
20	23	1	Fact	1	-1	1	10	90	1	1360
21	22	1	Fact	-1	0	1	5	90	1	1151
22	24	1	Fact	1	0	1	15	90	1	1669.5
23	11	1	Axial	0	-1	0	10	60	0.5	903
24	21	1	Fact	1	-1	1	15	60	1	1434.5
25	9	1	Fact	1	1	-1	15	120	0	1545
26	2	1	Fact	0	-1	-1	10	60	0	599
27	28	1	Fact	0	0	0	10	90	0.5	1080
28	6	1	Fact	1	0	-1	15	90	0	1155
29	1	1	Fact	-1	-1	-1	5	60	0	342
30	3	1	Fact	1	-1	-1	15	60	0	875
31	15	1	Axial	1	0	0	15	90	0.5	1397.5
32	31	1	Fact	0	0	0	10	90	0.5	1080

Table 3 – ANOVA (Partial sum of square) for total damping force (F)

Source	Sum of squares	d.f.	Mean square	F-value	Prob>F	Remark
Model	4365178	9	485019.7354	255.865	< 0.0001	Significant
A-A-Amplitude	1930613	1	1930612.5	1018.466	< 0.0001	Significant
B-B-RPM	790443.6	1	790443.5556	416.9868	< 0.0001	Significant
C-C-Current	1505691	1	1505690.889	794.3049	< 0.0001	Significant
AB	107541.3	1	107541.3333	56.73183	< 0.0001	Significant
AC	7752.083	1	7752.083333	4.089497	0.0555	
BC	638.0208	1	638.0208333	0.336578	0.5677	
A^2	17807.78	1	17807.77502	9.394227	0.0057	
B^2	2.640405	1	2.640405294	0.001393	0.9706	

C^2	874.9481	1	874.9480976	0.461566	0.5040	
Residual	41703.38	22	1895.60825			
Lack of Fit	41703.38	17	2453.140088			
Pure Error	0	5	0			
Cor Total	4406881	31				
Std. Dev.	43.53858		R-Squared	0.990537		
Mean	1102.25		Adj R-Squared	0.986665		
C.V. %	3.949974		Pred R-Squared	0.976504		
PRESS	103545.1		Adeq Precision	67.89797		

III. RNESULTS AND DISCUSSION

Table 2 shows all values of total damping force. The total damping force was obtained in the range of 342 N to 2070 N.

The increase in total damping force is due to

- Increasing of applied current value, which increases the shear stress of MR fluid.
- Increasing of angular speed, which increases the velocity of piston.
- Increasing of amplitude, this is also due to large displacement of fluid inside the piston cylinder assembly.

Fig. 8-10 shows relation between total damping force (measured force in N) with applied current values, angular speed and amplitude for different combinations. The rate of increasing in total damping force is higher for increasing the value of current compare to amplitude and velocity. Fig. 8 also shows that the total damping force is increased linearly with respect to increase in value of applied current. This observation agrees well with results reported by previous researchers. [13, 14, 15, 17, 20]

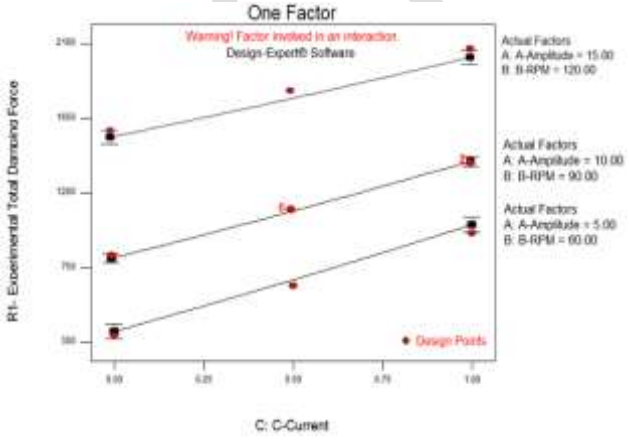

Fig. 8 – Total measured damping force vs. applied current at different values of amplitude and angular speed.

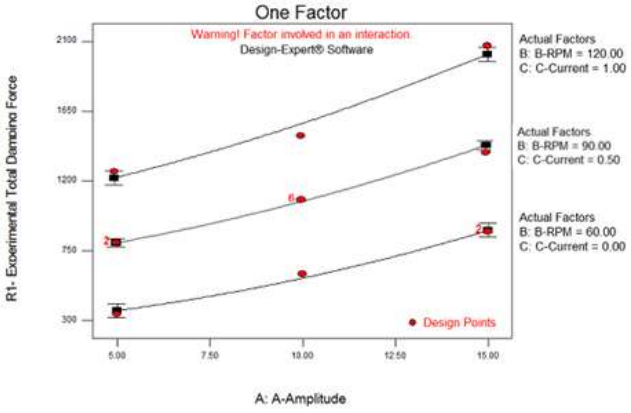

Fig. 9 – Total measured damping force vs. Amplitude at various angular speed and applied current.

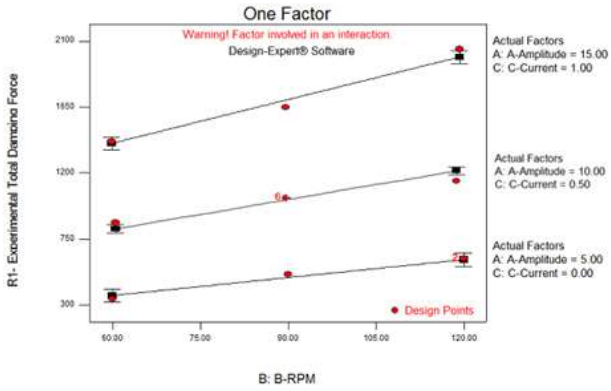

Fig. 10 – Total measured damping force vs. Angular velocity at various amplitude and applied current.

Furthermore, the results were analysed in Design Expert V6 software. The results of the block 1 experiments in the form of analysis of variance (ANOVA) are presented. An ANOVA summary table is commonly used to summarize the test of the regression model, test of the significance factors and their interaction and lack-of-fit test. If the value of 'Prob > F' in ANOVA table is less than 0.05 then the model, the factors, interaction of factors and curvature are said to be significant

Table 3 shows that the model is significant and amplitude (A), angular speed (B), applied current (C) and (A, B) are only the significant factors (terms) in the model. All other terms are insignificant. The contribution of factors, their interaction and curvature is also shown in Table 3.

The various R2 statistics (i.e. R2, adjusted R2 (R2 Adj) and predicted R2 (R2 Pred)) of the total damping force Table 3. The value of R2 = 0.990537 for total damping force indicates that 99.05% of the total variations are explained by the model. The adjusted R2 is a statistic that is adjusted for the "size" of the model; that is, the number of factors (terms). The value of the R2 Adj = 0.986665 indicates that 98.66% of the total variability is explained by the model after considering the significant factors. R2 Pred = 0.976504 is in good agreement with the R2 Adj and shows that the model would be expected to explain 97.65% of the variability in new data (Montgomery, 2001). 'C.V.' stands for the coefficient of variation of the model and it is the error expressed as a percentage of the mean ((S.D./Mean) ×100). Lower value of the coefficient of variation (C.V. = 3.9%) indicates improved precision and reliability of the conducted experiments. As curvature (nonlinearity) is not present in the model, additional experiments are not required to be performed. This is the main advantage of sequential approach in face cantered central composite design.

The normal probability plot of the residuals (i.e. error = predicted value from model−actual value) for Total damping Force is shown in Fig. 11, reveal that the residuals lie reasonably close to a straight line, giving support that terms mentioned in the model are the only significant (Montgomery, 2001).

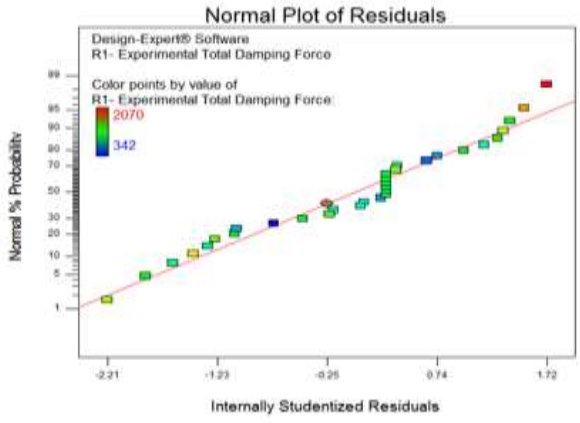

Fig. 11 Normal probability plot of residuals for Total Damping Force data.

After removing the insignificant factors, the response surface equations for Total damping Force is obtained in the actual values as follows:

Total Measured damping Force

$$F = -26.1306 * A + 1.038635 * B + 679.6246 + 0.631111 * A * B - 10.1667 * A * C - 0.48611 * B * C + 1.995699 * A^2 - 0.00068 * B^2 + 44.23656 * C^2 + 195.8705$$

Where

F = Total damping force in N
A = Amplitude value in mm
B = Angular Speed value in RPM
C = Applied Current value in Amp.

The predicted values from the model (equation value) and the actual (experimental) values are shown in Fig. 12.

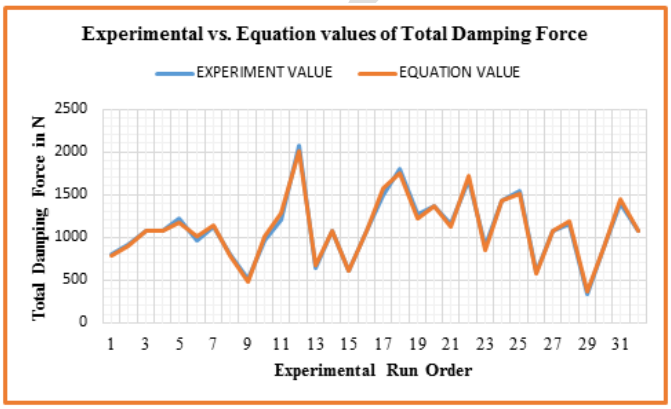

Fig. 12 – Actual vs. predicted values of total damping forces.

Since variable damping force is required for replacing the passive vibration control system to a semi-active vibration control system. The major focus of research is to find out total damping force for which desired damping coefficient can be achieved. Hence, the contour plots of the total damping force with relation in amplitude of vibration, angular velocity of vibrating device and applied current to MR damper are essential. The contour plot of the total damping force in angular velocity-amplitude at current value of 0.5 amp, current-amplitude at angular velocity value of 90 RPM, and current-angular velocity at amplitude value of 10 mm are shown in Figs 13-15, respectively. Figs. 13-15 clearly show that a good total damping force can be achieved for any level of amplitude and angular velocity, when current value is changed from low to high. In present research work, the MR fluid based semi-active damper is designed to achieve variable damping force by changing the current value.

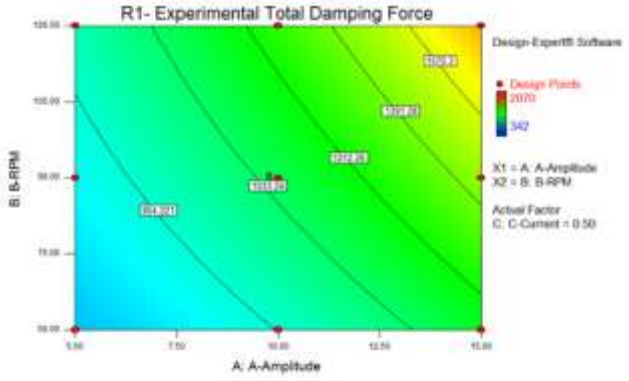

Fig. 13 – Measured Damping Force (N) contour in Angular speed (RPM) and Amplitude (mm) plane at current value of 0.5 Amp.

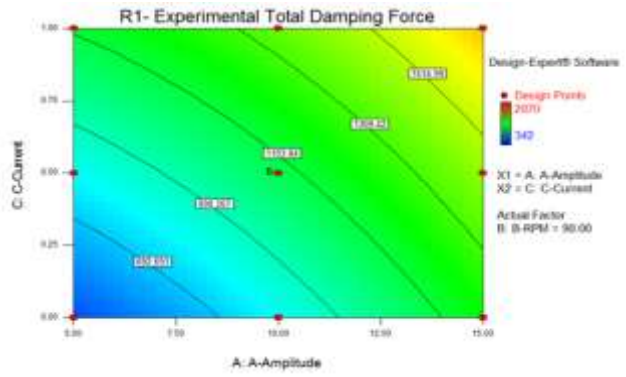

Fig. 14 – Measured Damping Force (N) contour in current (Amp) and Amplitude (mm) plane at Angular speed of 90 RPM.

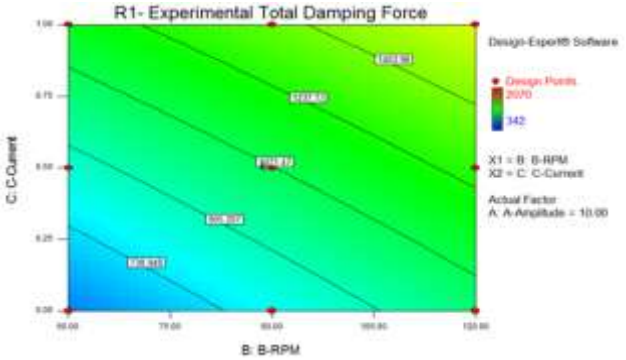

Fig. 15 – Measured Damping Force (N) contour in current (Amp) and Angular speed (RPM) plane at Amplitude of 10 mm.

IV. Conclusion

This paper presents the findings of an experimental investigation of the effect of velocity of damper piston, amplitude of damping system and applied current value to damper on the total damping force developed by damping system of developed MR fluid based damper for this research project and following conclusions are drawn. Sequential approach in central composite design is beneficial as it saves number of experimentations required. This was observed in total damping force analysis.

- Quadratic model is fitted for total damping force.
- All the factors (piston velocity, Amplitude and Current) has significant effect on Total Damping Force.
- The applied current is most significant factor, by which the value of total damping force can be adjusted according to system requirement. Thus the current provides primary contribution and influences most significantly on the total damping force. The interaction between amplitude and velocity provide secondary contribution to the model.
- High value of total damping force can be achieved when amplitude, velocity and current values are set nearer to their high level of the experimental range (15mm, 120 RPM and 1.0 A respectively).
- Contour plots can be used for selecting the parameters for providing the given desired total damping force.
- Experimental results of the developed damper are in good agreement with the predicted (equation) values.

REFERENCES

[1]. Karnopp D, Crosby M.J, Farwood R.A (1974) Vibration control using semi-active force generators. ASME j. eng. ind. 96(2): 619-626.

[2]. Yi K, Song B.S (1999) A new adaptive sky-hook control of vehicle semi-active suspensions. Proc. of IMechE, Part D: j. auto. eng. 213(3): 293-303.

[3]. Kawashima K, Unjoh S, Shimizu K (1992) Experiments on Dynamics Characteristics of Variable Damper. Proc. of the japan national symp. On structural response control, Tokyo, Japan: 121.

[4]. Mizuno T, Kobori T, Hirai J, Matsunaga Y, Niwa N (1992) Development of Adjustable Hydraulic Dampers for Seismic Response Control of Large Structure. ASME PVP conf.: 163-170.

[5]. Mark R Jolly, J David Carlson and Beth C Munoz (1996) A model of the behaviour of magnetorheological materials", Smart Mater. Struct. 5 (1996) 607–614.

[6]. Rabinow J (1948) Proceedings of the AIEE trans. 67: 1308-1315.

[7]. Rabinow J (1951) US Patent 2,575,360.

[8]. Carlson J.D, Chrzan M.J (1994) Magnetorheological Fluid Dampers. U.S. Patent 5277281.

[9]. Carlson J.D, Weiss K.D (1994) A growing attraction to magnetic fluids. J. Machine design 66(15): 61-64.

[10]. S.J Dyke, Spencer B.F. Jr, Sain M.K, Carlson J.D (1996) Modelling and control of magneto-rheological fluid dampers for seismic response reduction. Smart material and structures 5: 565-575.

[11]. Boelter R., Janocha H (1998) Performance of long-stroke and low-stroke MR fluid damper. Proc. of SPIE, smart structures and materials: passive damping and isolation, San Diego, CA: 303-313.

[12]. Carlson J.D, Jolly M.R (2000) MR fluid, foam and elastomer devices. Mechatronics 10: 555-569.

[13]. Hong S.R, Choi S.B, Choi Y.T, Wereley N.M (2005) Non-dimensional analysis and design of a magnetorheological damper. J. of sound vib. 288(4): 847-863.

[14]. Choi K.M, Jung H.J, Cho S.W, Lee I.W (2007) Application of smart passive damping system using MR damper to highway bridge structure. KSME Int. j. 21(6): 870-874.

[15]. Spelta C, Previdi F, Savaresi S.M, Fraternale G, Gaudiano N (2009) Control of magnetorheological dampers for vibration reduction in a washing machine. Mechatronics 19(3): 410-421.

[16]. Spencer B.F, Dyke S.J, Sain M.K, Carlson J.D (1996) Phenomenological Model of a Magneto-Rheological Damper. ASCE J. of eng. mech. 123(3): 230-238.

[17]. Choi S.B, Lee S.K (2001) A Hysteresis Model for the Field-dependent Damping Force of a Magneto-rheological Damper. J. of sound vib. 245(2): 375-383.

[18]. Dominguez A, Sedaghati R, Stiharu I (2004) Modelling the hysteresis phenomenon of magnetorheological dampers. Smart mat. struc. 13(6): 1351–1361.

[19]. D.I. Lalwani, N.K. Mehta, P.K. Jain (2007), Experimental investigations of cutting parameters influence on cutting forces and surface roughness in finish hard turning of MDN250 steel. Journal of materials processing technology (Elsevier) 206 (2008) 167–179

[20]. Heon-Jae Lee, Seok-Jun Moonb, Hyung-Jo Junga, Young-Cheol Huhb, Dong-Doo Janga –Korea(2008) Integrated Design Method of MR damper and Electromagnetic Induction System for Structural Control, Sensors and Smart Structures Technologies for Civil, Mechanical, and Aerospace Systems 2008, SPIE Vol. 6932 69320S-2